

Solution doping of organic semiconductors using air-stable n-dopants

Yabing Qi, Swagat K. Mohapatra, Sang Bok Kim, Stephen Barlow, Seth R. Marder et al.

Citation: *Appl. Phys. Lett.* **100**, 083305 (2012); doi: 10.1063/1.3689760

View online: <http://dx.doi.org/10.1063/1.3689760>

View Table of Contents: <http://apl.aip.org/resource/1/APPLAB/v100/i8>

Published by the [American Institute of Physics](#).

Related Articles

Tuning the interfacial hole injection barrier between p-type organic materials and Co using a MoO₃ buffer layer
J. Appl. Phys. **112**, 033704 (2012)

Triisopropylsilylethynyl-functionalized anthradithiophene derivatives for solution processable organic field effect transistors
Appl. Phys. Lett. **101**, 043301 (2012)

The high-pressure electronic structure of the [Ni(ptdt)₂] organic molecular conductor
J. Chem. Phys. **137**, 024701 (2012)

Functional K-doping of eumelanin thin films: Density functional theory and soft x-ray spectroscopy experiments in the frame of the macrocyclic protomolecule model
J. Chem. Phys. **136**, 204703 (2012)

Exciton transport in organic semiconductors: Förster resonance energy transfer compared with a simple random walk
J. Appl. Phys. **111**, 044510 (2012)

Additional information on *Appl. Phys. Lett.*

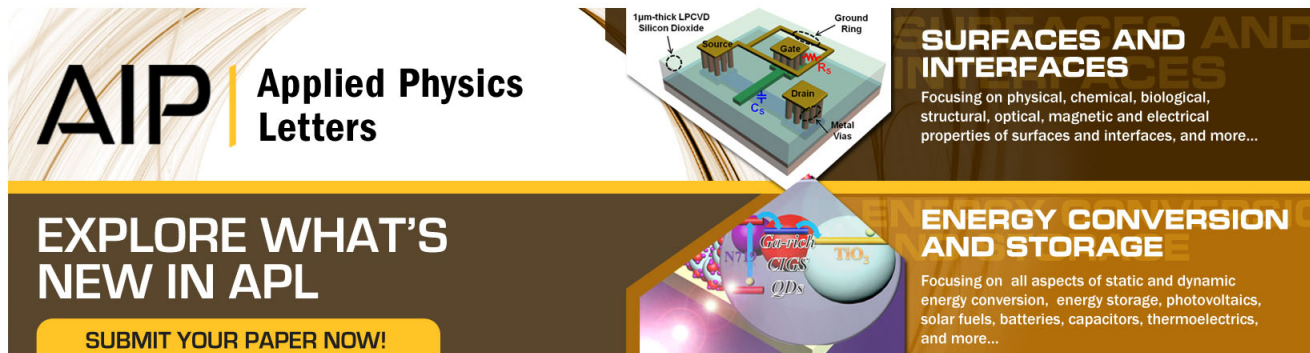
Journal Homepage: <http://apl.aip.org/>

Journal Information: http://apl.aip.org/about/about_the_journal

Top downloads: http://apl.aip.org/features/most_downloaded

Information for Authors: <http://apl.aip.org/authors>

ADVERTISEMENT



AIP | Applied Physics
Letters

EXPLORE WHAT'S NEW IN APL

SUBMIT YOUR PAPER NOW!

SURFACES AND INTERFACES
Focusing on physical, chemical, biological, structural, optical, magnetic and electrical properties of surfaces and interfaces, and more...

ENERGY CONVERSION AND STORAGE
Focusing on all aspects of static and dynamic energy conversion, energy storage, photovoltaics, solar fuels, batteries, capacitors, thermoelectrics, and more...

Solution doping of organic semiconductors using air-stable n-dopants

Yabing Qi,^{1,a),b)} Swagat K. Mohapatra,² Sang Bok Kim,² Stephen Barlow,² Seth R. Marder,² and Antoine Kahn^{1,a)}

¹Department of Electrical Engineering, Princeton University, Princeton, New Jersey 08544, USA

²Center for Organic Photonics and Electronics and School of Chemistry and Biochemistry, Georgia Institute of Technology, Atlanta, Georgia 30332-0400, USA

(Received 31 January 2012; accepted 6 February 2012; published online 24 February 2012)

Solution-based n-doping of the polymer poly{[N,N'-bis(2-octyldodecyl)-naphthalene-1,4,5,8-bis(dicarboximide)-2,6-diyl]-alt-5,5'-(2,2'-bithiophene)} [P(NDI₂OD-T₂)] and the small molecule 6,13-bis(tri-(isopropyl)silylethynyl)pentacene (TIPS-pentacene) is realized with the air-stable dimers of rhodocene, [RhCp₂]₂, and ruthenium(pentamethylcyclopentadienyl)(1,3,5-triethylbenzene), [Cp**Ru*(TEB)]₂. Fermi level shifts, measured by direct and inverse photoemission spectroscopy, and orders of magnitude increase in current density and film conductivity point to strong n-doping in both materials. The strong reducing power of these air-stable dopants is demonstrated through the n-doping of TIPS-pentacene, a material with low electron affinity (3.0 eV). Doping-induced reduction of the hopping transport activation energy indicates that the increase in film conductivity is due in part to the filling of deep gap states by carriers released by the dopants. © 2012 American Institute of Physics. [<http://dx.doi.org/10.1063/1.3689760>]

Chemical doping of organic semiconductors has been shown to be an effective method to circumvent issues of low material conductivity and inefficient charge injection.¹ Charges transferred from the dopants fill, and effectively remove, deep states in the gap of the organic host^{2,3} and increase the carrier concentration, thereby enhancing carrier mobility and film conductivity. Doping enables the control of energetic barriers to electron transfer at organic/electrode⁴ and organic/organic⁵ interfaces, leading to the possibility of ohmic contacts and low operating voltages for organic devices.⁶ Key criteria for selecting dopants are (1) the ability to p- or n-dope materials with a given ionization energy (IE) or electron affinity (EA), respectively, (2) diffusional stability, and (3) air-stability and solution processability for non-vacuum processing.^{1,7-10} In that regard, the air stability of powerful n-dopants is a particularly challenging issue given the facile oxidation of reducing agents with IE lower than ~4.0 eV.¹⁰⁻¹⁸ Previous attempts to address this problem made use of stable precursors, such as pyronin B (Refs. 15 and 19) or rhodamine B salts. However, this type of approach has yet to dope challenging low-EA electron-transport materials and generally suffers from the detrimental incorporation of non-doping by-products in the organic film. Air-stable benzoimidazole derivatives have been used to n-dope fullerene derivatives, e.g., [6,6]-Phenyl-C61-butyric acid methyl ester (PCBM), in solution,¹⁰ yet again the doping ability demonstrated to date is limited to compounds with EA ≥ 4.0 eV. We present here the results obtained for solution doping of two compounds, the electron-transport polymer poly{[N,N'-bis(2-octyldodecyl)-naphthalene-1,4,5,8-bis(dicarboximide)-2,6-diyl]-alt-5,5'-(2,2'-bithiophene)},

(P(NDI₂OD-T₂); Ref. 20) and 6,13-bis(triisopropylsilylethynyl)pentacene (TIPS-pentacene; Ref. 21) with the dimers of rhodocene, [RhCp₂]₂, and ruthenium(pentamethylcyclopentadienyl)(1,3,5-triethylbenzene), [Cp**Ru*(TEB)]₂ (Figure 1). We recently showed that dimers of this type are relatively stable in air, yet clearly undergo reactions with acceptors in which electrons are transferred and C—C bonds cleaved to afford the corresponding monomeric cations and the acceptor radical anion.²² In this paper, we demonstrate that efficient n-doping is achieved in both P(NDI₂OD-T₂), an electron-transport polymer with sufficiently large EA (3.95 eV) for air-stable electronics, and TIPS-pentacene, which is typically used for hole-transport and presents a far greater challenge for n-doping (EA ~ 3.0–3.1 eV).

[RhCp₂]₂ and [Cp**Ru*(TEB)]₂ (Figure 1) were synthesized as previously described.²² These solid compounds were exposed to ambient air for significant periods of time (hours) prior to being used; we have shown that such exposure results in no detectable decomposition according to ¹H NMR spectroscopy. P(NDI₂OD-T₂) (Polyera) and TIPS-pentacene (Sigma Aldrich) were used as host materials. A 9:1 mixture of TIPS-pentacene and polystyrene (PS) (Sigma Aldrich) was used to improve the film morphology (hereafter called TIPS:PS). Undoped and doped thin films (thickness 10–20 nm for electron spectroscopy and 50–100 nm for transport measurements) were prepared by spin coating in a N₂ glove box, using a simple semiconductor-dopant co-solution method to control the doping ratio. P(NDI₂OD-T₂) and TIPS:PS were dissolved in chlorobenzene and toluene, respectively. We have previously determined the rate law and rate constant for the solution reaction of [Cp**Ru*(TEB)]₂ and TIPS-pentacene.²² Under the pseudo-first-order conditions of the current solution doping procedure, where the concentration of TIPS-pentacene is large and effectively constant, the half-life of the dimeric dopant can be estimated as ca. 2 min at room temperature. Accordingly, under the conditions used for solution preparation prior to spin coating

^{a)}Authors to whom correspondence should be addressed. Electronic addresses: yabing.qi@oist.jp and kahn@princeton.edu.

^{b)}Present address: Energy Materials and Surface Sciences Unit, Okinawa Institute of Science and Technology, Graduate University, 1919-1 Tancha, Onna-son, Kunigami-gun, Okinawa 904-0495, Japan.

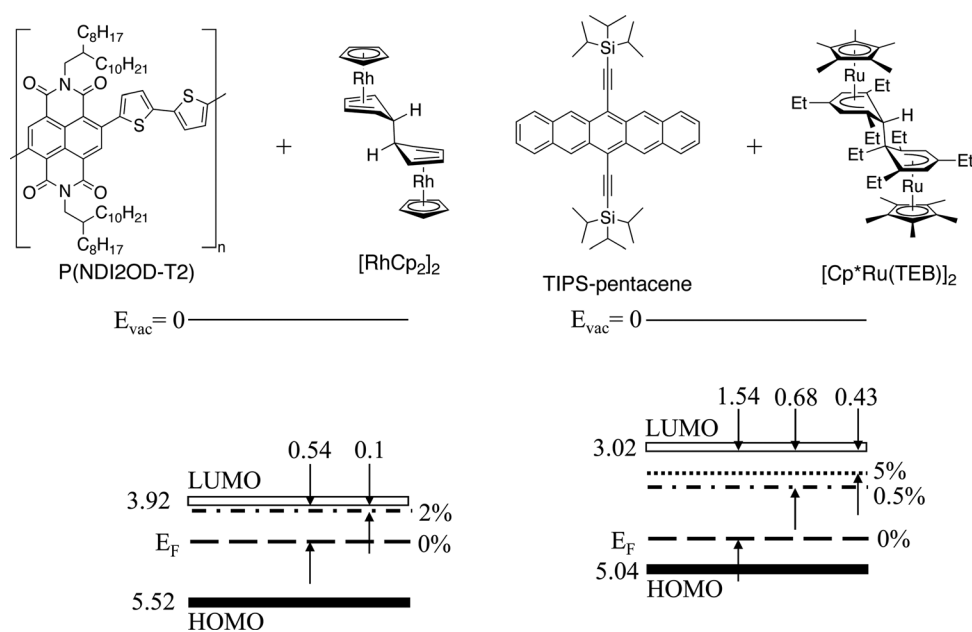


FIG. 1. Left panel: (top) Chemical structures of P(NDI₂OD-T₂) and [RhCp₂]₂; (bottom) energy diagram of P(NDI₂OD-T₂) showing HOMO and LUMO positions relative to the vacuum level and the Fermi level as a function of doping concentration of [RhCp₂]₂ (all energies are in eV). Right panel: Same as left, for TIPS-pentacene and [Cp^{*}Ru(TEB)]₂.

(10 min sonication at room temperature and 15 min at 90 °C), the reaction should be effectively complete. The reaction of [RhCp₂]₂ and P(NDI₂OD-T₂) is expected to be even more rapid owing to the lower barrier estimated (based on electrochemical data) for this reaction. Thus, effectively all the dopant molecules are expected to participate in doping in both cases. Conducting substrates (Au/Si or ITO) were used for in-vacuum electron spectroscopy and for simple current-voltage (I-V) diode measurements in N₂ performed with a Hg probe. The Au substrates were cleaned in solvents, whereas ITO surfaces were cleaned and treated with oxygen plasma. Quartz substrates prepared with a pattern of interdigitated Au electrodes were used for in-vacuum variable-temperature I-V (VTIV) transport measurements. Ultraviolet photoemission spectroscopy (UPS) and inverse photoemission spectroscopy (IPES) were performed in ultra-high vacuum to determine IE, EA, and work function (WF) of all undoped and doped films. Measurement resolutions in UPS and IPES were 0.15 eV and 0.45 eV, respectively. The position of the Fermi level (E_F) was determined with both techniques by measuring the Fermi step on a bare Au sample.

Detailed UPS and IPES spectra (not shown here) were recorded for P(NDI₂OD-T₂) spin-coated on Au, undoped, or doped with 2 wt. % [RhCp₂]₂, and for TIPS:PS spin-coated on ITO, undoped, or doped with either 0.5 or 5 wt. %

[Cp^{*}Ru(TEB)]₂. The P(NDI₂OD-T₂) IE, EA, and single-particle gap are found to be 5.52 eV, 3.92 eV, and 1.60 eV, respectively, in good agreement with previously reported values.^{20,23} The TIPS:PS IE (5.04 eV) and EA (3.02 eV) are found to be very close to those of pentacene,²⁴ however, at variance with previously reported values of 5.8 eV and 4.8 eV, respectively.²⁵ Upon doping, the P(NDI₂OD-T₂) and TIPS:PS spectrum line shapes remain unchanged except for a rigid shift toward higher binding energy. This is equivalent to an upward movement of E_F in the gap, indicative of n-doping. The results are summarized in Figure 1. Most relevant to the current study, the energy difference between the bottom edge of the LUMO and E_F, measured with the combination of UPS and IPES, decreases from 0.54 eV to 0.1 eV upon doping P(NDI₂OD-T₂) with 2 wt. % [RhCp₂]₂ and from 1.54 eV to 0.68 eV and 0.43 eV upon doping TIPS:PS with 0.5 and 5 wt. % [Cp^{*}Ru(TEB)]₂, respectively. The initial E_F position in the undoped film is not particularly significant, as it depends on the nature and work function of the substrate. However, the significance lies in the movement of E_F upon doping and its ultimate position in the gap of the semiconductor.

I-V characteristics of the undoped and doped films, measured in N₂ with a Hg probe, are shown in Figures 2(a) and 2(b). In the P(NDI₂OD-T₂) case, the current density in

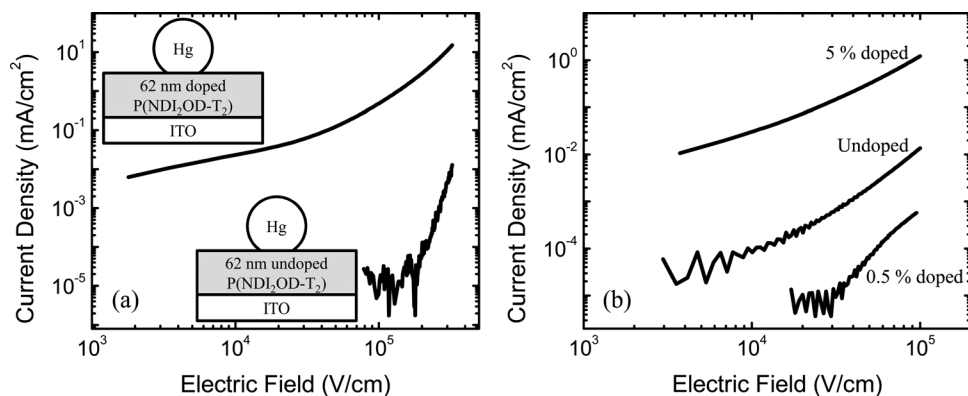


FIG. 2. Current density–electric field (J–F) characteristics for (a) undoped and 2 wt. % [RhCp₂]₂ doped P(NDI₂OD-T₂) samples, and (b) undoped and 0.5 wt. %, 5 wt. % [Cp^{*}Ru(TEB)]₂ doped TIPS:PS blend (9:1) samples.

the doped sample (2 wt. % [RhCp₂]₂) (positive bias on Hg, electrons injected from ITO) is enhanced by several orders of magnitude, depending on the bias (e.g., 5×10^4 times for a field of 2×10^5 V/cm). In the low-field ohmic conduction regime ($J \propto V$), the doped films sustain a strong current density. The slope of the current increases with injection and trap-filling at fields higher than 3×10^4 V/cm. The current in the undoped films is too low to be measured with our set-up below 100 kV/cm (< 10 pA).

In TIPS:PS (Figure 2(b)), the evolution of the current with doping is more complex. Undoped TIPS-pentacene is a hole transport material. With positive bias on Hg, the current is dominated by holes injected from Hg (work function ~ 4.5 eV) rather than electrons injected from ITO (work function 4.7–4.8 eV). The energy diagram of Figure 1 shows the large electron injection barrier at the TIPS:PS/ITO interface. The hole injection barrier at the Hg contact, although not measured directly, is presumed to be ~ 0.7 – 0.8 eV. When the film is n-doped with only 0.5 wt. % [Cp**Ru*(TEB)]₂, E_F moves upward in the gap, increasing hole barriers at both Hg and ITO contacts and leading to a current drop. As the dopant concentration increases to 5 wt. %, the semiconductor becomes n-doped, E_F approaches the LUMO, and the current switches to electrons injected at the ITO electrode. The data recorded for negative bias applied to Hg (not shown here) show precisely the same trend. Note that this type of transition from hole- to electron-dominated current was already observed in the case of another hole-transport material, i.e., copper phthalocyanine (CuPc) n-doped with decamethylcobaltocene (CoCp₂*).¹¹

To further explore transport vs. T in doped P(NDI₂OD-T₂), VTIV measurements were performed on both undoped and doped (2 wt. % [RhCp₂]₂) P(NDI₂OD-T₂) films. Transport is in the plane parallel to the film, between Au electrodes separated by 150 μ m, making the contact resistance irrelevant and allowing measurement of the bulk conductivity of the material. The applied voltage ranged from -50 to 50 V, with maximum field of 3.3 kV/cm. For the doped samples, I-V curves were recorded for temperatures ranging between 170 K and 410 K (the current was too low for reliable measurement below 170 K), and were found to be linear over the entire field range. The undoped samples were measured only between 350 K and 410 K because of their lower conductivity and gave linear I-V curves over the entire field range. The conductivity plots ($\ln(\sigma)$ vs. T) of the undoped and doped films, extracted from the linear fits to the I-V curves, are shown in Figure 3. As expected, the doped samples are orders of magnitude more conductive than the undoped samples. The conductivity of the doped samples reaches 5.1×10^{-4} S/cm at room temperature. In both cases, the conductivity follows a simple Arrhenius dependence on temperature, from which an activation energy (E_a) can be extracted for the hopping transport, $\sigma = \sigma_0 e^{-\frac{E_a}{kT}}$, where σ_0 is a constant prefactor. E_a equals 1.19 eV for undoped P(NDI₂OD-T₂) and 0.23 eV for the 2 wt. % doped film.

Similar drops in E_a were previously reported for hole-transport materials α -NPD p-doped with tris[1,2-bis(trifluoromethyl)-ethane-1,2-dithiolene] (Mo(tfd)₃) (Ref. 26) and pentacene p-doped with 2,3,5,6-tetrafluoro-7,7,8,8-tetracyanoquinodimethane (F₄-TCNQ).²⁷ The large activation energy in

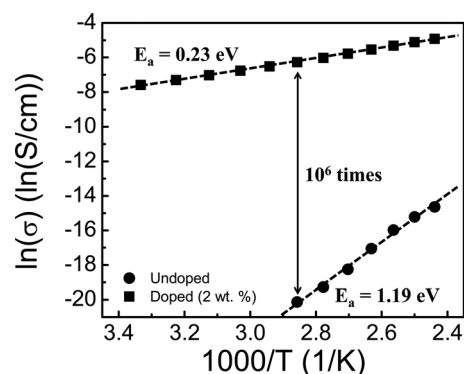


FIG. 3. $\ln(\sigma)$ vs. $1000/T$ for undoped (circles) and doped (squares) P(NDI₂OD-T₂) films. Activation energy values are extracted from the linear fits to the curves.

the undoped material results from the presence of disorder (static and dynamic) and impurity-related states extending deep above the HOMO edge in the electronic gap, which trap carriers. Doping fills these traps with holes, rendering them electronically inactive. In the P(NDI₂OD-T₂) case, the current is dominated by electrons and the process presumably involves electron trapping in deep states below the LUMO edge. As in the hole-case, defects play a key role. Oxygen- and water-related traps are also known to affect electron transport in these materials. The abrupt decrease in E_a upon doping is entirely consistent with the filling of these trap states by electrons released on oxidation and cleavage of the dimer. Electron transport then occurs in/from states significantly closer to the mobility edge, with much lower activation energy, a phenomenon also observed in poly[2-methoxy-5-(2-ethylhexyloxy)-1,4-phenylenevinylene] (MEH-PPV) n-doped with decamethylcobaltocene.³ However, it should be noted that conductivity is a product of both the density of carriers and their mobility, and it is still unclear how much of the conductivity increase in the present case is due to each of these two components.

In summary, we demonstrated n-doping of the polymer P(NDI₂OD-T₂) and the small molecule TIPS-pentacene via co-solution with the air-stable [RhCp₂]₂ and [Cp**Ru*(TEB)]₂ dimers, respectively. The reducing power of these dopants is evidenced by the effective n-doping of TIPS-pentacene, a host with a 3.0 eV electron affinity. The dopants are converted to the monomeric cations RhCp₂⁺ and Cp**Ru*(TEB)⁺, respectively.²² Doping and increase in conductivity are demonstrated via electron spectroscopy and room and low temperature I-V measurements. The (orders of magnitude) increase in conductivity is the result of a combination of doping-induced filling of deep electron trap states in the material and increase in the density of available carriers.

This material is based on work supported by Solvay S.A., the Office of Naval Research (N00014-11-1-0313), and the National Science Foundation (DMR-1005892 and through the Science and Technology Center Program, DMR-0120967).

¹K. Walzer, B. Maennig, M. Pfeiffer, and K. Leo, *Chem. Rev.* **107**, 1233 (2007).

²Y. Qi, T. Sajoto, S. Barlow, E.-G. Kim, J.-L. Brédas, S. R. Marder, and A. Kahn, *J. Am. Chem. Soc.* **131**, 12530 (2009).

- ³Y. Zhang, B. de Boer, and P. W. M. Blom, *Phys. Rev. B* **81**, 085201 (2010).
- ⁴W. Gao and A. Kahn, *Org. Electron.* **3**, 53 (2002).
- ⁵W. Gao and A. Kahn, *Appl. Phys. Lett.* **82**, 4815 (2003).
- ⁶X. Zhou, M. Pfeiffer, J. Blochwitz, A. Werner, A. Nollau, T. Fritz, and K. Leo, *Appl. Phys. Lett.* **78**, 410 (2001).
- ⁷S.-G. Chen, H. M. Branz, S. S. Eaton, P. C. Taylor, R. A. Cormier, and B. A. Gregg, *J. Phys. Chem. B* **108**, 17329 (2004).
- ⁸W. Gao and A. Kahn, *J. Appl. Phys.* **94**, 359 (2003).
- ⁹J. Hwang and A. Kahn, *J. Appl. Phys.* **97**, 103705 (2005).
- ¹⁰P. Wei, J. H. Oh, G. Dong, and Z. Bao, *J. Am. Chem. Soc.* **132**, 8852 (2010).
- ¹¹C. K. Chan, W. Zhao, S. Barlow, S. Marder, and A. Kahn, *Org. Electron.* **9**, 575 (2008).
- ¹²M.-H. Chen and C.-I. Wu, *J. Appl. Phys.* **104**, 113713 (2008).
- ¹³F. Li, A. Werner, M. Pfeiffer, K. Leo, and X. Liu, *J. Phys. Chem. B* **108**, 17076 (2004).
- ¹⁴A. Nollau, M. Pfeiffer, T. Fritz, and K. Leo, *J. Appl. Phys.* **87**, 4340 (2000).
- ¹⁵A. G. Werner, F. Li, K. Harada, M. Pfeiffer, T. Fritz, and K. Leo, *Appl. Phys. Lett.* **82**, 4495 (2003).
- ¹⁶J. H. Oh, P. Wei, and Z. Bao, *Appl. Phys. Lett.* **97**, 243305 (2010).
- ¹⁷S. Tanaka, E. Kawabe, K. Kanai, T. Iwahashi, T. Nishi, Y. Ouchi, and K. Seki, *J. Electron Spectrosc. Relat. Phenom.* **144–147**, 533 (2005).
- ¹⁸A. Werner, F. Li, K. Harada, M. Pfeiffer, T. Fritz, K. Leo, and S. Machill, *Adv. Funct. Mater.* **14**, 255 (2004).
- ¹⁹C. K. Chan, E. G. Kim, J. L. Brédas, and A. Kahn, *Adv. Funct. Mater.* **16**, 831 (2006).
- ²⁰H. Yan, Z. Chen, Y. Zheng, C. Newman, J. R. Quinn, F. Dotz, M. Kastler, and A. Facchetti, *Nature* **457**, 679 (2009).
- ²¹R. Hamilton, J. Smith, S. Ogier, M. Heeney, J. E. Anthony, I. McCulloch, J. Veres, D. D. C. Bradley, and T. D. Anthopoulos, *Adv. Mater.* **21**, 1166 (2009).
- ²²S. Guo, S. B. Kim, S. K. Mohapatra, Y. Qi, T. Sajoto, A. Kahn, S. R. Marder, and S. Barlow, *Adv. Mater.* **24**, 699 (2012).
- ²³Z. Chen, Y. Zheng, H. Yan, and A. Facchetti, *J. Am. Chem. Soc.* **131**, 8 (2008).
- ²⁴C. Chan and A. Kahn, *Appl. Phys. A* **95**, 7 (2009).
- ²⁵O. L. Griffith, J. E. Anthony, A. G. Jones, and D. L. Lichtenberger, *J. Am. Chem. Soc.* **132**, 580 (2010).
- ²⁶Y. Qi, T. Sajoto, M. Kröger, A. M. Kandabarow, W. Park, S. Barlow, E.-G. Kim, L. Wielunski, L. C. Feldman, R. A. Bartynski *et al.*, *Chem. Mater.* **22**, 524 (2010).
- ²⁷S. D. Ha, Y. Qi, and A. Kahn, *Chem. Phys. Lett.* **495**, 212 (2010).